ISSN PRINT 2319 1775 Online 2320 7876

Research paper UGC CARE Listed (Group -I) Journal Volume 11,S Iss 12, Dec 2022

Design and Performance Analysis of Super Critical Fluid Extraction for SC-CO_2

Dr. Nookala Venu

Professor, Department of Electronics and Communication Engineering, Balaji Institute of Technology and Science, Warangal -506 331, Telangana, India

Corresponding Author Mail id: venunookala@gmail.com

Abstract

A simple mathematical model to characterise the supercritical extraction process has been proposed in this paper. This model is primarily based on two mass transfer mechanisms: solubility and diffusion. The model assumes two districts mode of extraction: initial constant rate extraction that is controlled by solubility and falling rate extraction that is controlled by diffusivity. Effects of extraction parameters such as pressure and temperature on the extraction of oil have also been studied. The proposed model, when compared with existing models, shows better agreement with the experimental results. The proposed model developed has been applied for both high initial oil content material and low initial oil content material.

Key words: *Supercritical fluid extraction, Mass transfer, Carbon dioxide, Cashew nut shells, Black pepper*

1. Introduction

Extraction of natural products using super critical carbon dioxide (SC-CO_2) offers significant benefits, such as reduced environmental pollutions, better recovery of components, improved product quality, etc. over other conventional extraction methods. The process design and simulation of supercritical fluid extraction (SCFE) of natural products requires both qualitative and quantitative understanding of mass transfer kinetics. During extraction of natural products, solute dissolves into the super critical solvent. The rate of extraction depends on the nature of oil within the plant cells. If solute is freely available on the outer surface of the seeds, extraction process is simple. On the other hand, as solute interacts with the cell matrix, extraction becomes difficult. Mass transfer kinetics depends on different process parameters, particle size of the seed, and amount of easily accessible oil. Several models have been proposed to study the mass transfer kinetics. venu et al. [1-5] assumed that the mass transfer resistance occurred only in the solvent phase. Essentially, this model assumes that only easily extractable oil can be extracted. venu et al. [6-9] used a shrinking core leaching model to describe a variable external mass transfer resistance where the solute balance in the solid phase determines the thickness of the mass transfer layer in external part of the oil seeds. It is assumed that the oil interacts with the cell matrix and hence, it is not easily extractable. venu et al. [10-14] recognized a distinction in solid phase between broken cells and intact cells to model the desorption equilibrium as a limiting step during extraction of essential oils using SC-CO_2. venu et al. [15-20] proposed the broken-intact cell model, which requires the internal mass transfer coefficient as an adjustable parameter. They have calculated the other parameters from the experimental data. venu et al. [21-23] gave a model with external mass transfer and the equilibrium between solvent and solute as the controlling step.

The limitations of the shrinking core leaching model lies in the fact that it requires five adjustable parameters: fluid film mass transfer coefficient, desorption rate constant, adsorption equilibrium constant, axial diffusivity, and the effective diffusivity in the porous solid. Out of these parameters, at least two parameters are regressed from the

ISSN PRINT 2319 1775 Online 2320 7876

Research paper UGC CARE Listed (Group -I) Journal Volume 11,S Iss 12, Dec 2022

experimental results while the others are obtained from the available correlations. Accuracy of this model, therefore, depends on the correlations used. The broken-intact cell model proposed by venu et al. [24-28] requires only internal mass transfer coefficient as an adjustable parameter. However, the limitation of this model is that the cell structure data required for solution of the model, are obtained by scanning electron microscope (SEM) images and requires expertise to avoid any confusion between the oil bearing cells and biological cells (starch bearing cells). This model does not give the accurate results for the seeds having very low initial oil contents. SEM analysis of the microstructure shows that it cannot develop specialized oil-bearing structure for the seeds with very low initial oil content. The model proposed by venu et al. [29-32] has three adjustable parameters: partition factor, overall mass transfer coefficient, and adsorption equilibrium constant. The limitation of this model lies in the fact that adsorption equilibrium constant has been correlated within given temperature range of their work. In fact adsorption equilibrium constant increases with increase in solubility. At constant pressure, increase in temperature decreases density of SC-CO_2 and simultaneously increases volatility of the solute. As a result, solubility of solute depends on the larger contribution of one of the two effects mentioned above. Hence, correlation of adsorption equilibrium constant as a function of temperature proposed by venu et al. [33-38] may not be true for temperature that is outside the range mentioned in their work.

venu et al. [39-42] considered the solid phase as divided between broken and intact cells. They distinguished the total oil available within the plant cell in easily accessible oil and oil present in the intact cell. venu et al. [43-46] described the extraction curves by three-step procedure. The first linear portion is denoted by constant extraction rate (CER) period and is characterized by the convective mass transfer between the solid material surface and the fluid phase. Supercritical solvent carries easily accessible oil from broken plant cells during this phase.

2. Mathematical Model

Supercritical fluid (SCF) is used as a solvent for the selective separation of the components present in the natural products in SCFE. The liquid like density of a SCF solvent provides its high solvent power, whereas the gas like diffusivity and viscosity impart excellent transport properties, which in turn enhances the mass transfer rate as compared to that of liquid organic solvent. The solid feed particles in the extractor are considered to be stationery as the flow rate of the SCF is very low and the extraction process is carried out in a fixed-bed condition. As super critical carbon dioxide (SC-CO_2) flows through the void spaces of the feed material, solute gets dissolved in it. The extraction process can be primarily divided into following two distinct sections.

(i) Initial CER section where the easily accessible solute available on the external surface of the feed particles gets extracted. In this section solubility of the solute controls the extraction rate.

(ii) FER section where the easily accessible oil gets depleted and the diffusion mechanism controls the extraction process.

It is assumed that the easily accessible solute is completely depleted at the extractor entrance at the end of CER period.

The flowing solvent may get saturated with the solute after traversing a short bed height initially, beyond which it is not possible to extract any further. Therefore, the concentration of solute in the SCF solvent at the exit of bed is at the highest in the beginning of the extraction and may remain steady for some time before the concentration starts

ISSN PRINT 2319 1775 Online 2320 7876

Research paper UGC CARE Listed (Group -I) Journal Volume 11,S Iss 12, Dec 2022

falling. This saturation line moves in the direction of flow and reaches the exit of the bed after some time. The constant rate period depends on the flow rate of the solvent and the characteristics of the solid substrate. For certain natural material containing low extractable oil there is no initial constant rate period [47-50]. In this case the rate of mass transfer takes place at the falling rate regime and is controlled by internal diffusion resistance. The transition from a constant rate regime to a falling rate regime depends on the initial oil content in the solid substrate as well as the cell structure of the natural material. The model assumes that the solvent flows axially at a constant superficial velocity through a fixed bed of cylindrical shape. The solvent is pure at the entrance of the extractor. The temperature and pressure are kept constant throughout the fixed bed. In addition, the bed is assumed to be homogeneous in terms of solute distribution as well as particle size. The model also assumes pseudo-steady state with plug flow, and neglects the accumulation of the solute in the fluid phase. It takes into account the solute solubility in the solvent and mass transfer coefficient both in solvent and in solid phases.

Solid phase and fluid phase mass balances for a bed element is given as

$$-\rho_s(1-\varepsilon)\frac{\partial x}{\partial t} = J(x,y) \tag{1}$$

$$\rho_f U\frac{\partial y}{\partial h} = J(x,y) \tag{2}$$

The cellulose structure of the plant cell consists of the strongly packed solute. During grinding or milling of the plant material, the cell wall breaks and some portion of the solute become loose (easily accessible oil) while the remaining solute (oil present in the intact cell) is still strongly packed within the cell structure. Therefore, out of the total initial solute content, x_0 , the amount of solute inside the particles is x_k. Solute contents are expressed as solute free solid phase basis. At the beginning of the extraction, oil concentration throughout the bed is x_0 . The SCF enters the bottom of the extractor and starts extracting solute from the feed material. The concentration of the solute in the solvent at the entrance of the extractor is zero. The concentration of the solute in the flowing SCF increases in the direction of the flow in the extractor and reaches to the maximum at the extractor exit. This can be mathematically expressed as (initial conditions)

$$x(h, t=0) = x_0 \tag{3a}$$

$$y(h=0, t) = 0 \tag{3b}$$

During the initial phase of extraction, solvent carries easily accessible oil available on the outer surface of the broken cells. The mass transfer mechanism is controlled by the solubility of the solvent at the extractor operating condition. The mass transfer rate depends on the concentration of solute in the solvent. It decreases along the flow direction of the solvent as concentration of solute in solvent increases in that direction. This mechanism prevails till the concentration of the oil reaches to x_k at the entrance of the extractor. The mass transfer rate may be expressed as

$$J(x,y) = k_f a_o \rho_f (y_r - y) \quad \text{For } x > x_k \tag{4}$$

In literature, several expressions for mass transfer rate of supercritical fluid extraction have been proposed. venu *et al*. [51], venu et al. [52], venu et al. [53] and venu et al. [54] described the mass transfer rate in the CER period by

ISSN PRINT 2319 1775 Online 2320 7876

Research paper UGC CARE Listed (Group -I) Journal Volume 11,S Iss 12, Dec 2022

equation (4). On the other hand, different authors have proposed different models for the mass transfer rate for the diffusion-controlled region. venu et al. [55] described the mass transfer rate as a function of internal mass transfer resistance and solute concentration in the solid phase. They have not considered the effect of solubility of solvent at different operating parameters. venu et al. [56] and venu et al. [57] proposed a model with solute concentration in solid phase and solubility as model parameters. venu et al. [58] considered external mass transfer co-efficient even for diffusion-controlled region. In fact, internal mass transfer coefficient controls the extraction in the diffusion region. venu et al. [59] considered internal mass transfer coefficient for the slow extraction period. In the proposed model, the effect of internal mass transfer resistance and solute concentration in solid phase has been considered for FER period. The relation proposed for mass transfer rate during the FER period in this work is due to the fact that the solvent phase concentration varies with the concentration of solute in feed material, *x*.

$$J(x,y) = k_s a_o \rho_s x \quad \text{For } x \le x_k \tag{5}$$

2.1. Model Solution

For $x > x_k$ the fluid phase mass balance may be expressed by combining equations (2) and (4).

$$\rho_f U \frac{\partial y}{\partial h} = k_f a_0 \rho_f \left(y_r - y\right) \tag{6}$$

Introducing the dimensionless variables such as dimensionless concentration of solute in solid phase $r = x / x_k$, normalized dimensionless concentration of the solute in solvent phase $Y = 1 - y / y_r$, dimensionless time $\tau = k_f a_0 \rho_f y_r t / \rho_s x_k (1-\varepsilon)$, and dimensionless height $\alpha = k_f a_0 h / u$, equation (6) can be written as

$$\frac{\partial Y}{\partial \alpha} = -Y \tag{7}$$

Integrating above equation with initial conditions (3) gives the concentration profile of solute in solvent along the bed height,

$$Y = \exp(-\alpha) \tag{8}$$

Similarly, the solid phase mass balance is expressed as

$$\frac{\partial r}{\partial \tau} = -Y \tag{9}$$

Solution of equation (9) with initial conditions (3) yields

$$r = r_0 - \tau \exp(-\alpha) \tag{10}$$

Equation (10) gives the concentration of solute inside the solid particles at a given instant and given bed height. The oil content in solid substance of the extractor in the CER period is equal to the difference of initial oil content in the feed material and the oil carried away by the solvent till that time. Therefore, the extraction curve maybe determined as,

ISSN PRINT 2319 1775 Online 2320 7876

Research paper UGC CARE Listed (Group -I) Journal Volume 11,S Iss 12, Dec 2022

$$e = x_0 - \frac{1}{H}\int_0^H x dh = x_0 - \frac{x_k}{A}\int_0^A r d\alpha \tag{11}$$

Where $A = k_f a_0 H / u$.

The extraction curve may be expressed to indicate the amount of solute carried away by specific amount of supercritical fluid. The extraction curve as a function of specific amount of the solvent *q*, can be expressed as

$$e = q y_r \left[1 - \exp(-A)\right] \quad \text{For } q < q_m \tag{12}$$

Where $q_m = \left(x_0 - x_k\right) / y_r A$.

As the easily accessible oil gets depleted at the extractor entrance with the specific amount of solvent q_m, the transition between CER and FER period occurs. At the start of FER period, the extraction from inside the particles takes place near the extractor entrance section. However, the easily accessible solute is still present at the other section of extractor. After some time, extraction process is entirely controlled by the diffusion phenomenon. The concentration of the solute in feed material at the transition period between the CER and FER period can be written as the difference between the initial oil content on solute-free solid basis and the amount of extract carried away with the specific amount of solvent, q_m.

$$\text{At } \tau = \tau_m,\ r = r_0 - \tau_m \exp(-\alpha) \tag{13}$$

For $x < x_k$, the solid phase mass balance is written as,

$$\frac{\partial r}{\partial \tau} = -Kr \tag{14}$$

Where, $K = k_s \rho_s x_k / k_f \rho_f y_r$. Integration of above equation with initial conditions (13) gives the concentration of the solute in solute free solid phase in FER period.

$$r = \left(r_0 - \left(r_0 - 1\right)\exp(-\alpha)\right)\exp\left(-K\left(\tau - \tau_m\right)\right) \tag{15}$$

The extraction curve for FER period can be obtained using equation (11) as

$$e = x_0 - \exp\left\{-BA\left(q - q_m\right)\right\}\left[x_0 - q_m y_r \left(1 - \exp(-A)\right)\right] \quad \text{For } q \geq q_m \tag{16}$$

Where, $B = k_s \rho_s / k_f \rho_f$, and $A = k_f a_0 H / u = k_f a_0 \rho_f / \dot{q}(1-\varepsilon)\rho_s = F / \dot{q}$.

Parameter *A* is function of fluid phase mass transfer coefficient and specific flow rate of the solvent for the given particle size and operating parameters (extraction pressure and temperature). It increases with increase in fluid phase mass transfer coefficient and decreases with specific flow rate of the solvent. On the other hand, parameter B is function of both fluid phase and solid phase mass transfer coefficients for the given operating parameters. It represents the role of solubility and diffusivity in controlling the extraction phenomenon in the FER period. It can be seen from equation (16) that with increase in parameter *A* cumulative yield of solute increases. Applications of the proposed model are discussed in the following section.

3. Application of the model

ISSN PRINT 2319 1775 Online 2320 7876

Research paper UGC CARE Listed (Group -I) Journal Volume 11,S Iss 12, Dec 2022

The proposed model is applied for the yield prediction at different operating parameters for the CNS and Black pepper. The selection of the material is made on the basis of the total initial oil content. CNS contains about 40 to 45% (w/w) of oil where as black pepper contains hardly 7 to 8 % (w/w) of oil.

3.1. Application of the model for CNS

The set of experiments were carried out to study the effect of operating parameters on the extraction of CNSL. The experimental methodology is explained in detail elsewhere [60]. About 100 gm of CNS with mesh size 8 were taken in the extractor. The feed material was kept under equilibrium at given operating parameters for about 1 hr. Then, SC-CO_2 was expanded through metering valve to atmospheric pressure and the extract was collected in the separator. The mass of CO_2 released was calculated on the basis of the extractor volume, CO_2 density at extractor parameters and density of CO_2 at atmospheric pressure. In the first set, the temperature and mass flow rate of solvent were kept constant at 333 K and 2.777×10^{-4} kg/s respectively, while pressure was changed from 250 to 300 bar in the step of 25 bar. Second set of experiments was carried out with change in temperature from 313 to 333 K in the step of 10 K with constant mass flow rate and density. Here pressures were modified to get constant density of 830 kg/m^3 at respective temperatures.

To determine the maximum amount of oil present in the feed material, about 100 gm of CNS were taken into the extractor. The pressure, temperature and mass flow rate of the solvent were set at 300 bar, 333 K and 1 kg/h and the experiment was extended for about 16 hours. In order to find the oil present in the residue, the residue was pyrolysed as per the method suggested by venu [60]. The volatiles from the pyrolysis reactor were condensed and the oil condensed was calculated by gravimetric method. The total initial oil content in feed was calculated by the sum of the oil obtained by SCFE and pyrolysis method. It was found that the initial oil concentration was 30% by weight of original biomass, while on the basis of solute free solid, it was 42.85%. The mass transfer based parameter F and B were obtained by regressing the experimental results. The amount of solvent required for the extraction of oil during constant extraction rate period, q_m, is calculated directly from the formula derived in the last section.

Table 1 shows the values of model parameters of the proposed model obtained using the experimental data for CNS. It may be noted that the fluid phase mass transfer coefficient (F) increases with the increase in extraction pressure and temperature. It is due to the fact that solubility of solvent increases with increase in pressure and density. At higher solubility the mass transfer rates are higher, and hence CER ends earlier. However, it was found that the solute collected during the CER period for all the cases was same in the order of 35% of the initial oil content in the seed. This behavior compliments the fact that for the same particle size the amount of easily accessible oil for the given seed structure, and hence the value of x_k is same. For the parametric study it was decided to grind the CNS particles to the size of mesh 8. Due to higher initial content of oil, CNSL oozes out during the grinding process. The milled seed particles get wetted with oil and tend to agglomerate and hence make it difficult to maintain the uniform particle size of the ground seed material. The value of x_k was found to be 0.11. The model proposed by venu [61] was also used to obtain the mass transfer parameters. It was found that the values of regressed parameters of the proposed model were of the same order of magnitude. The model proposed also used to obtain the mass transfer parameters. It was found that the values of regressed parameters were of the same magnitude. The model proposed

ISSN PRINT 2319 1775 Online 2320 7876

Research paper **© 2012 IJFANS. All Rights Reserved,** UGC CARE Listed (Group -I) Journal Volume 11,S Iss 12, Dec 2022

in this work gave better accuracy (on the basis of the values of average absolute relative deviation (AARD)) in comparison to venu [62] model. The AARD indicates that the model predicted results are in good agreement with experimental results.

3.2. Application of the model for Black pepper

The proposed model was used to validate the experimental results published by venu et al. [63]. The data were obtained for the extraction of black pepper (Piper nigrum L.) essential oil in the temperature range of 303 K to 323 K and pressure range of 150 to 300 bar. The data were obtained for two different types of ground black pepper (batches 1 and 2). The solubility of black pepper in SC-CO_2, initial oil concentration inside the particles and the solvent flow rate at given operating parameter were taken from the values are reported.

Table 1 shows the comparison of the model parameters for proposed model and venu et al. [64] model. It is observed that fluid phase mass transfer co-efficient, *F*, for both the models are comparable in most of the cases. For the given operating parameters and a batch, the mass transfer co-efficient increases with the increase in either pressure or mass flow rate of the solvent or both. The AARD for the yield predicted by both the models have been presented in Table 2. The results predicted by the proposed model are in agreement with venu [65] model. Figure 1 compares the experimental and predicted overall extraction curves for the pepper from batch 2. It shows that the results predicted by the proposed model are comparable with the experimental results. It is interesting to note here that the proposed model is predicting results as accurately as predicted by venu [66] model in spite of the fact that proposed model considers only two sections as compared to three sections in venu [66] model for the extraction curve.

Figure 3 compares the predicted and experimental overall extraction curves at 313 K for different operating parameters. Here, it may be observed that the model predicts the experimental results with reasonable accuracy. The effect of extraction pressure, solvent flow rate and pre-treatment of the material is well appreciated in Figure 1. At 300 bar and with higher mass flow rate of solvent, the extraction of pepper from batch 1 is quite faster as compared to pepper from batch 2. This may be due to the fact that, the initial oil content of pepper from batch 2 is very less. On the other hand, it can be seen from Figure 1(a) that at lower pressure, pepper from batch 2 gives quite higher yield as compared to pepper from batch 1. This may be attributed to higher solvent flow rate in the former as compared to later.

ISSN PRINT 2319 1775 Online 2320 7876

Research paper UGC CARE Listed (Group -I) Journal Volume 11,S Iss 12, Dec 2022

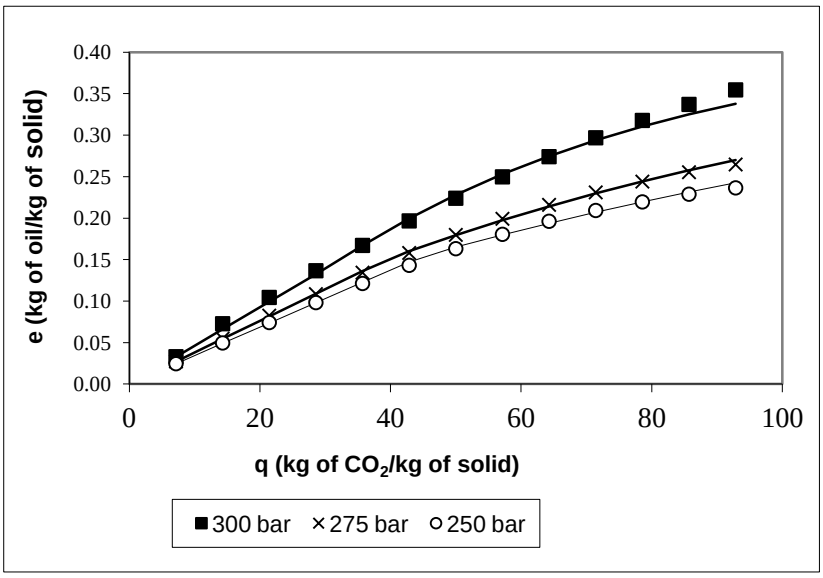

(a)

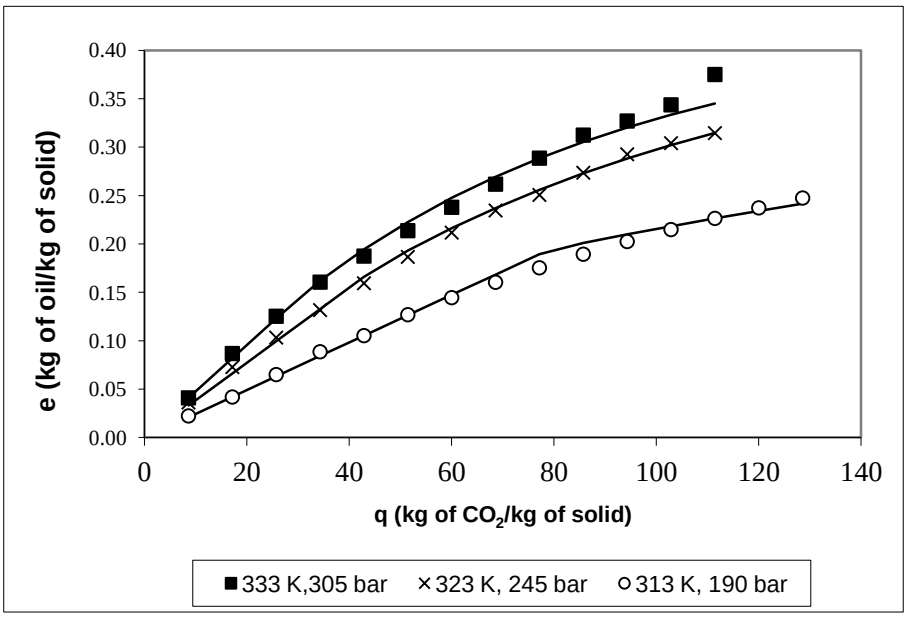

(b)

Fig.1 Overall extraction curves for CNSL at solvent flow rate 2.777×10^{-4} kg/s and

(a) Extractor temperature 333 K (b) solvent density of 830 g/l.

(b) Experimental results are shown as symbols. Predicted extraction curves are shown as solid curves.

Table 1: Parameters for the proposed model based on experimental results of extraction of CNSL from CNS.

ISSN PRINT 2319 1775 Online 2320 7876

Research paper UGC CARE Listed (Group -I) Journal Volume 11,S Iss 12, Dec 2022

P/T/m (bar/K/kg/hr)	*A*	y_r (kg oil/ kg solvent)	q_m (kg solvent /kg solid)	*B*	Proposed model		Existing model	
					AARD (%)	Max. error	AARD (%)	Max. error
300/333/1	1.8408	0.0055	31	0.01008	2.61	9.02	3.01	10.68
275/333/1	1.7506	0.0046	39	0.00601	0.74	1.97	1.60	3.62
250/333/1	1.6978	0.0042	44	0.00478	1.01	2.77	2.16	4.39
305/333/1.2	1.7388	0.0058	30	0.00864	2.94	8.01	7.49	14.81
245/323/1.2	1.3641	0.0052	44	0.00886	2.83	8.29	6.85	10.50
190/313/1.2	1.0907	0.0037	78	0.00420	2.97	6.18	4.12	8.68

4. Conclusion

A simple mathematical model has been proposed that explains the complete extraction curve in two sections only. The model proposed is based on the fundamental mass transfer operations: solubility and diffusion. Proposed model is applicable to supercritical extraction of different biomass. Results for CNSL and black pepper oil show that the model agrees well with the experimental results for the seeds having both high as well as low initial oil contents. The comparison of the proposed model results with the venu et.al model [64] results indicate that the accuracy of proposed model is of same order though the proposed model is simplified by considering two-section kinetics as against three section kinetics in venu et.al [65] model. The mass transfer coefficient was found an order of magnitude higher for CNS than black pepper. The AARD for both the materials was in the range of 1 to 5 %. At present, the work is being done to apply the model for techno-economic feasibility study and scale-up.

References

[1] Nookala Venu, S. K. (2022). Machine Learning Application for Medicine Distribution Management System. IJFANS, 11 (1), 2323-2330.

[2] Vaigandla, K. K., & Venu, D. N. (2021). A survey on future generation wireless communications-5G: multiple access techniques, physical layer security, beamforming approach. *Journal of Information and Computational Science*, *11*(9), 449-474.

[3] Venu, D., Arun Kumar, A., & Vaigandla, K. K. (2022). Review of Internet of Things (IoT) for Future Generation Wireless Communications. *International Journal for Modern Trends in Science and Technology*, *8*(03), 01-08.

[4] Sujith, A. V. L. N., Swathi, R., Venkatasubramanian, R., Venu, N., Hemalatha, S., George, T., ... & Osman, S. M. (2022). Integrating nanomaterial and high-performance fuzzy-based machine learning approach for green energy conversion. *Journal of Nanomaterials*, *2022*, 1-11.

[5] Venu, N., & Anuradha, B. (2013, December). Integration of hyperbolic tangent and Gaussian kernels for fuzzy C-means algorithm with spatial information for MRI segmentation. In *2013 Fifth International Conference on Advanced Computing (ICoAC)* (pp. 280-285). IEEE.

[6] Vaigandla, K. K., & Venu, D. N. (2021). Ber, snr and papr analysis of ofdma and sc-fdma. GIS Science Journal, ISSN, (1869-9391), 970-977.

[7] Venu, N. (2014, April). Performance and evalution of Guassian kernals for FCM algorithm with mean filtering based denoising for MRI segmentation. In *2014 International Conference on Communication and Signal Processing* (pp. 1680-1685). IEEE.

ISSN PRINT 2319 1775 Online 2320 7876

Research paper **© 2012 IJFANS. All Rights Reserved,** UGC CARE Listed (Group -I) Journal Volume 11,S Iss 12, Dec 2022

[8] Vaigandla, K. K., & Venu, D. (2021). Survey on Massive MIMO: Technology, Challenges, Opportunities and Benefits.

[9] Venu, N., & Anuradha, B. (2015). Multi-Kernels Integration for FCM algorithm for Medical Image Segmentation Using Histogram Analysis. *Indian Journal of Science and Technology*, *8*(34), 1-8.

[10] Venu, N., Yuvaraj, D., Barnabas Paul Glady, J., Pattnaik, O., Singh, G., Singh, M., & Adigo, A. G. (2022). Execution of Multitarget Node Selection Scheme for Target Position Alteration Monitoring in MANET. *Wireless Communications and Mobile Computing*, *2022*.

[11] Venu, N., Swathi, R., Sarangi, S. K., Subashini, V., Arulkumar, D., Ralhan, S., & Debtera, B. (2022). Optimization of Hello Message Broadcasting Prediction Model for Stability Analysis. *Wireless Communications & Mobile Computing (Online)*, *2022*.

[12] Venu, D. N. Analysis of Xtrinsic Sense MEMS Sensors. *International Journal of Advanced Research in Electrical, Electronics and Instrumentation Engineering (IJAREEIE), ISSN*, 2278-8875.

[13] Venu, N., & Anuradha, B. (2013). A novel multiple-kernel based fuzzy c-means algorithm with spatial information for medical image segmentation. *International Journal of Image Processing (IJIP)*, *7*(3), 286.

[14] Nookala Venu, A. (2018). Local mesh patterns for medical image segmentation. *Asian Pacific Journal of Health Sciences*, *5*(1), 123-127.

[15] Venu, N., & Anuradha, B. (2013). PSNR Based Fuzzy Clustering Algorithms for MRI Medical Image Segmentation. *International Journal of Image Processing and Visual Communication*, *2*(2), 01-07.

[16] Thouti, S., Venu, N., Rinku, D. R., Arora, A., & Rajeswaran, N. (2022). Investigation on identify the multiple issues in IoT devices using Convolutional Neural Network. *Measurement: Sensors*, *24*, 100509.

[17] Venu, N., Revanesh, M., Supriya, M., Talawar, M. B., Asha, A., Isaac, L. D., & Ferede, A. W. (2022). Energy Auditing and Broken Path Identification for Routing in Large-Scale Mobile Networks Using Machine Learning. *Wireless Communications and Mobile Computing*, *2022*.

[18] Kesavaiah, D. C., Goud, T. R., Rao, Y. S., & Venu, N. (2019). Radiation effect to MHD oscillatory flow in a channel filled through a porous medium with heat generation. *Journal of Mathematical Control Science and Applications*, *5*(2), 71-80.

[19] Venu, N., & Anuradha, B. (2015). Medical Image Segmentation Using Kernal Based Fuzzy C Means Algorithm. *Research Scholar, Dept. of ECE, SVU College of Engineering, Sri Venkateswara University, Tirupati-517502, India*, *4*(1).

[20] Nookala Venu, D., Kumar, A., & Rao, M. A. S. (2022). BOTNET Attacks Detection in Internet of Things Using Machine Learning. *Neuroquantology*, *20*(4), 743-754.

[21] Venu, N., & Anuradha, B. (2014, February). Multi-Hyperbolic Tangent Fuzzy C-means Algorithm for MRI Segmentation. In *Proceedings of International Conference on Advances in Communication, Network and Computing (CNC-2014), Elsevier* (pp. 22-24).

[22] Nookala Venu, S. W. (2022). A Wearable Medicines Recognition System using Deep Learning for People with Visual Impairment. *IJFANS*, *12*(1), 2340-2348.

[23] Venu, D., Rakesh, G., Maneesha, K., Anusha, K., Merugu, S., & Mohammad, A. (2022). Smart Road Safety and Vehicle Accidents Prevention System for Mountain Road. *International Journal from Innovative Engineering and Management Research (IJIEMR)*.

[24] Nookala Venu, D., Kumar, A., & Rao, M. A. S. (2022). Smart Agriculture with Internet of Things and Unmanned Aerial Vehicles. *Neuroquantology*, *20*(6), 9904-9914.

[25] Nookala Venu, D., Kumar, A., & Rao, M. A. S. (2022). Internet of Things Based Pulse Oximeter For Health Monitoring System. *NeuroQuantology*, *20*(5), 5056-5066.

[26] Venu, D. N. DA (2021). Comparison of Traditional Method with watershed threshold segmentation Technique. *The International journal of analytical and experimental modal analysis*, *13*, 181-187.

[27] Vaigandla, K. K., & Venu, D. (2021). Survey on Massive MIMO: Technology. *Challenges, Opportunities and Benefits*.

ISSN PRINT 2319 1775 Online 2320 7876

Research paper **© 2012 IJFANS. All Rights Reserved,** UGC CARE Listed (Group -I) Journal Volume 11,S Iss 12, Dec 2022

[28] Kesavaiah, D. C., Goud, T. R., Venu, N., & Rao, Y. S. (2021). MHD Effect on Convective Flow Of Dusty Viscous Fluid With Fraction In A Porous Medium And Heat Generation. *Journal of Mathematical Control Science and Applications*, *7*(2).

[29] Babu, K. R., Kesavaiah, D. C., Devika, B., & Venu, D. N. (2022). effect on MHD free convective heat absorbing Newtonian fluid with variable temperature. *NeuroQuantology*, *20*(20), 1591-1599.

[30] Kesavaiah, D. C., Ahmed, M., Reddy, K. V., & Venu, D. N. (2022). Heat and mass transfer effects over isothermal infinite vertical plate of Newtonian fluid with chemical reaction. *NeuroQuantology*, *20*(20), 957-967.

[31] Reddy, G. B., Kesavaiah, D. C., Reddy, G. B., & Venu, D. N. (2022). A note on heat transfer of MHD Jeffrey fluid over a stretching vertical surface through porous plate. *NeuroQuantology*, *20*(15), 3472-3486.

[32] Chenna Kesavaiah, D., Govinda Chowdary, P., Rami Reddy, G., & Nookala, V. (2022). Radiation, radiation absorption, chemical reaction and hall effects on unsteady flow past an isothermal vertical plate in a rotating fluid with variable mass diffusion with heat source. *NeuroQuantology*, *20*(11), 800-15.

[33] Kesavaiah, D. C., Prasad, M. K., Reddy, G. B., & Venu, N. (2022). Chemical Reaction, Heat and Mass Transfer Effects on MHD Peristaltic Transport in A Vertical Channel Through Space Porosity And Wall Properties. *NeuroQuantology*, , *20*(11), 781-794.

[34] Kesavaiah, D. C., Reddy, G. B., Kiran, A., & Venu, D. N. (2022). MHD effect on boundary layer flow of an unsteady incompressible micropolar fluid over a stretching surface. *NeuroQuantology*, , *20*(8), 9442-9452.

[35] Kesavaiah, D. C., Chowdary, P. G., Chitra, M., & Venu, D. N. (2022). Chemical reaction and MHD effects on free convection flow of a viscoelastic dusty gas through a semi infinite plate moving with radiative heat transfer. *NeuroQuantology*, *20*(8), 9425-9434.

[36] Karne, R., Mounika, S., & Venu, D. (2022). Applications of IoT on Intrusion Detection System with Deep Learning Analysis. *International Journal from Innovative Engineering and Management Research (IJIEMR)*.

[37] Venu, N., & Anuradha, B. (2015). Two different multi-kernels for fuzzy C-means algorithm for medical image segmentation. *Int. J. Eng. Trends Technol.(IJETT)*, *20*, 77-82.

[38] Kesavaiah, D. C., Goud, T. R., Venu, N., & Rao, Y. S. (2017). Analytical Study on Induced Magnetic Field With Radiating Fluid Over A Porous Vertical Plate With Heat Generation. *Journal of Mathematical Control Science and Applications*, *3*(2).

[39] Venu, N., & Kumar, A. A. Routing and Self-Directed Vehicle Data Collection for Minimizing Data Loss in Underwater Network.

[40] Venu, N., & Kumar, A. A. Fuzzy Based Resource Management Approach for the Selection Of Biomass Material.

[41] Agarwal, R. K., Sahasrabuddhe, D., & Riyajuddin, A. A Novel Dates Palm Processing and Packaging Management System based on IoT and Deep Learning Approaches.

[42] Koshariya, A. K., Rout, S., & Venu, N. An Enhanced Machine Learning Approach for Identifying Paddy Crop Blast Disease Management Using Fuzzy Logic.

[43] Rout, S., & Venu, N. Machine Learning Based Analysis And Classification of Rhizome Rot Disease In Turmeric Plants.

[44] Jagadeesan, S., Barman, B., Agarwal, R. K., Srivastava, Y., Singh, B., Nayak, S. K., & Venu, N. A Perishable Food Monitoring Model Based on Iot And Deep Learning To Improve Food Hygiene And Safety Management. *interventions*, *8*, 9.

[45] Venu, N., Thalari, S. K., Bhat, M. S., & Jaiganesh, V. Machine Learning Application for Medicine Distribution Management System.

[46] Reddy, A. V., Kumar, A. A., Venu, N., & Reddy, R. V. K. (2022). On optimization efficiency of scalability and availability of cloud-based software services using scale rate limiting algorithm. *Measurement: Sensors*, *24*, 100468.

ISSN PRINT 2319 1775 Online 2320 7876

Research paper **© 2012 IJFANS. All Rights Reserved,** UGC CARE Listed (Group -I) Journal Volume 11,S Iss 12, Dec 2022

[47] Venu, D. (2022). Radiation Effect to Mhd Oscillatory Flow in a Channel Filled Through a Porous Medium with Heat Generation. *Radiation Effect to Mhd Oscillatory Flow in a Channel Filled Through a Porous Medium with Heat Generation (August 27, 2022). Research Article*.

[48] Venu, N. Smart Agriculture Remote Monitoring System Using Low Power IOT Network.

[49] Venu, N. IOT Surveillance Robot Using ESP-32 Wi-Fi CAM & Arduino.

[50] Venu, D., Soujanya, N., Goud, B. M., Bhavani, T. Y., & Rajashekar, A. (2022). Study and Experimental Analysis on FBMC and OFDM. *International Journal from Innovative Engineering and Management Research (IJIEMR)*.

[51] Katti, S. K., Ananthula, A., & Venu, D. (2022). Vehicle Fuel Level Monitor and Locate the Nearest Petrol Pumps Using IoT.

[52] Priya R, S., Tahseen, A., & Venu, D. (2022). Face Mask Detection System Using Python Open CV.

[53] Venu, D. (2022). Alcohol Detection and Engine Locking System. *International Journal from Innovative Engineering and Management Research (IJIEMR)*.

[54] Venu, D., Bindu, C., Srija, B., Maheshwari, V., Sarvu, S., & Rohith, S. (2022). Wireless Night Vision Camera on War Spying Robot. *International Journal from Innovative Engineering and Management Research (IJIEMR)*.

[55] Venu, N. IOT Based Enabled Parking System in Public Areas.

[56] Venu, N. IOT Based Speech Recognition System to Improve the Performance of Emotion Detection.

[57] Venu, N., & Sulthana, M. A. Local Maximum Edge Binary Patterns for Medical Image Segmentation.

[58] Venu, N. Design and intergration of different kernels for fuzzy means algorithm used for MRI medical image segmentation.

[59] Venu, N., & Anuradha, B. (2016). Multi-hyperbolic tangent fuzzy c-means algorithm with spatial information for MRI segmentation. *International Journal of Signal and Imaging Systems Engineering*, *9*(3), 135-145.

[60] Venu, N., & Anuradha, B. (2015). Hyperbolic Tangent Fuzzy C-Means Algorithm with Spatial Information for MRI Segmentation. *International Journal of Applied Engineering Research*, *10*(7), 18241-18257.

[61] Venu, N., & Anuradha, B. (2015, April). Two different multi-kernels integration with spatial information in fuzzy C-means algorithm for medical image segmentation. In *2015 International Conference on Communications and Signal Processing (ICCSP)* (pp. 0020-0025). IEEE.

[62] Venu, N., & Anuradha, B. (2015). MRI Image Segmentation Using Gaussian Kernel Based Fuzzy C-Means Algorithm.

[63] Venu, N., & Anuradha, B. (2015). Evaluation of Integrated Hyperbolic Tangent and Gaussian Kernels Functions for Medical Image Segmentation. *International Journal of Applied Engineering Research*, *10*(18), 38684-38689.

[64] Anita Tuljappa, V. N. (2022). Dufour and Chemical Reaction Effects on Two Dimensional incompressible flow of a Viscous fluid over Moving vertical surface. *NeuroQuantology* , 63-74.

[65] Ch. Achi Reddy, V. N. (2022). Magnetic Field And Chemical Reaction Effects on Unsteady Flow Past A Stimulate Isothermal Infinite Vertical Plate. *NeuroQuantology , 20* (16), 5360- 5373.

[66] Sowmya Jagadeesan, M. K. (2022). Implementation of an Internet of Things and Machine learning Based Smart Medicine Assistive System for Patients with Memory Impairment. *IJFANS International Journal of Food and Nutritional Sciences* , 1191-1202.